Inorg. Chem. **2007**, *46*, 3726–3735

C–H Cleavage and Double Alkyl Additions to the Disulfido Ligand in Dicyanido-Bridged Ru_2S_2 Complexes

Sumito Ishizu, Hiroyasu Sugiyama, Brian K. Breedlove,* and Kazuko Matsumoto*,†

Department of Chemistry, School of Science and Engineering, and Advanced Research Institute of Science and Engineering, Waseda University, 3-4-1 Okubo, Shinjuku, Tokyo 169-8555, Japan

Received December 22, 2006

Novel dicyanido-bridged dicationic $Ru^{III}SSRu^{III}$ complexes $[\{Ru(P(OCH_3)_3)_2\}_2(\mu\text{-}S_2)(\mu\text{-}X)_2\{\mu\text{-}m\text{-}C_6H_4(CH_2CN)_2\}](CF_3SO_3)_2$ (**4**, X = Cl, Br) were synthesized by the abstraction of the two terminal halide ions of $[\{RuX(P(OCH_3)_3)_2\}_2(\mu\text{-}S_2)(\mu\text{-}X)_2]$ (**1**, X = Cl, Br) followed by treatment with *m*-xylylenedicyanide. **4** reacted with 2,3-dimethylbutadiene to give the C_4S_2 ring-bridged complex $[\{Ru(P(OCH_3)_3)_2\}_2\{\mu\text{-}SCH_2C(CH_3)=C(CH_3)CH_2S\}(\mu\text{-}X)_2\{\mu\text{-}m\text{-}C_6H_4(CH_2CN)_2\}](CF_3SO_3)_2$ (**6**, X = Cl, Br). In addition, **4** reacted with 1-alkenes in CH_3OH to give alkenyl disulfide complexes $[\{Ru(P(OCH_3)_3)_2\}_2\{\mu\text{-}SS(CH_2C=CHR)\}(\mu\text{-}Cl)_2\{\mu\text{-}m\text{-}C_6H_4(CH_2CN)_2\}](CF_3SO_3)$ (**7**: R = CH_2CH_3, **9**: R = $CH_2CH_2CH_3$) and alkenyl methyl disulfide complexes $[\{Ru(P(OCH_3)_3)_2\}_2\{\mu\text{-}S(CH_3)S(CH_2C=HR)\}(\mu\text{-}Cl)_2\{\mu\text{-}m\text{-}C_6H_4(CH_2CN)_2\}](CF_3SO_3)_2$ (**8**: R = CH_2CH_3, **10**: R = $CH_2CH_2CH_3$) via the activation of an allylic C–H bond followed by the elimination of H^+ or condensation with CH_3OH. Additionally, the reaction of **4** with 3-penten-1-ol gave $[\{Ru(P(OCH_3)_3)_2\}_2\{\mu\text{-}SS(CH_2C=CHCH_2OH)\}(\mu\text{-}Cl)_2\{\mu\text{-}m\text{-}C_6H_4(CH_2CN)_2\}](CF_3SO_3)$ (**11**) via the elimination of H^+ and $[\{Ru(P(OCH_3)_3)_2\}_2(\mu\text{-}SCH_2CH=CHCH_2S)(\mu\text{-}Cl)_2\{\mu\text{-}m\text{-}C_6H_4(CH_2CN)_2\}](CF_3SO_3)_2$ (**12**) via the intramolecular elimination of a H_2O molecule. **12** was exclusively obtained from the reaction of **4** with 4-bromo-1-butene.

Introduction

C−H cleavage and C−S bond formation on the bridging-disulfide ligand in $[\{RuCl(P(OCH_3)_3)_2\}_2(\mu\text{-}S_2)(\mu\text{-}X)_2]$ (**1**) (X = Cl (**1-Cl**), Br (**1-Br**)) having the RuSSRu core has been developed by our group.[1−8] Free disulfur is too reactive toward a variety of substrates and unstable to study its reactivity directly; however, through the systematic study of **1** with unsaturated molecules, such as ketones,[3,4] alkenes,[5,6] alkynes,[7] and dienes,[8] the reactivity of the disulfido ligand in the Ru_2S_2 core has been established. From parent complex **1**, the dicationic complexes $[\{Ru(P(OCH_3)_3)_2(CH_3CN)\}_2(\mu\text{-}S_2)(\mu\text{-}Cl)_2]^{2+}$ (**2**) with a cis $Ru^{III}SSRu^{III}$ and $[\{Ru(P(OCH_3)_3)_2(CH_3CN)_3\}_2(\mu\text{-}S_2)]^{4+}$ (**3**) with a trans $Ru^{III}SSRu^{III}$ core were obtained by abstraction of chloride ions with the addition of 2 and 4 equiv of Ag^+, respectively. Because of the open cavity structure of the Ru_2S_2 core in **3** compared to **2**, **3** is reactive toward a wider variety of substrates. For instance, **2** undergoes only a Diels−Alder type cycloaddition to form a C_4S_2 ring moiety,[8] whereas **3** cleaves C−H bonds in various hydrocarbons to form C−S bonds with the disulfido ligand (Scheme 1). The differences in the electronic state and the structural difference of the Ru_2S_2 core affect the Lewis acidity of the disulfido ligand and cause the difference in reactivity. Several other systems are known that have also the $Ru^{III}SSRu^{III}$ core,[9−12] but these do not exhibit any reactivity on the disulfido ligand. Therefore, the co-ligands in **2** and **3** appear to be essential.

* To whom correspondence should be addressed. E-mail: brianbreedlove@hotmail.com (B.K.B), kmatsu@yf6.so-net.ne.jp (K.M).

† Present address: 3-9-12-105, Daizawa, Setagaya-ku, Tokyo 155-0032, Japan, Tel and Fax: +81-3-3413-5352.

(1) Matsumoto, T.; Matsumoto, K. *Chem. Lett.* **1992**, 559−562.
(2) Matsumoto, K.; Matsumoto, T.; Kawano, M.; Ohnuki, H.; Shichi, Y.; Nishide, T.; Sato, T. *J. Am. Chem. Soc.* **1996**, *118*, 3597−3609.
(3) Matsumoto, K.; Uemura, H.; Kawano, M. *Inorg. Chem.* **1995**, *34*, 658−662.
(4) Sugiyama, H.; Hossain, Md. M.; Lin, Y.-S.; Matsumoto, K. *Inorg. Chem.* **2000**, *39*, 3948.
(5) Hossain, Md. M.; Lin, Y.-S.; Sugiyama, H.; Matsumoto, K. *J. Am. Chem. Soc.* **2000**, *122*, 172−173.
(6) Sugiyama, H.; Hossain, Md. M.; Lin, Y.-S.; Matsumoto, K. *Inorg. Chem.* **2001**, *40*, 5547−5552.
(7) Sugiyama, H.; Moriya, Y.; Matsumoto, K. *Organometallics* **2001**, *20*, 5636−5641.
(8) Sugiyama, H.; Lin, Y.-S.; Matsumoto, K. *Angew. Chem., Int. Ed.* **2000**, *39*, 4058−4061.
(9) Brulet, C. R.; Ishied, S. S.; Taube, H. *J. Am. Chem. Soc.* **1973**, *95*, 4758.
(10) Elder, R. C.; Trukula, M. *Inorg. Chem.* **1977**, *16*, 1048.
(11) Amarasekera, J.; Rauchfuss, T. B.; Rheingold, A. L. *Inorg. Chem.* **1987**, *26*, 2017.
(12) Amarasekera, J.; Rauchfuss, T. B.; Wilson, S. R. *Inorg. Chem.* **1987**, *26*, 3328.

10.1021/ic062460k CCC: $37.00
Published on Web 03/29/2007

Scheme 1. Reactions of the Ru_2S_2 **2** and **3** with Organic Molecules

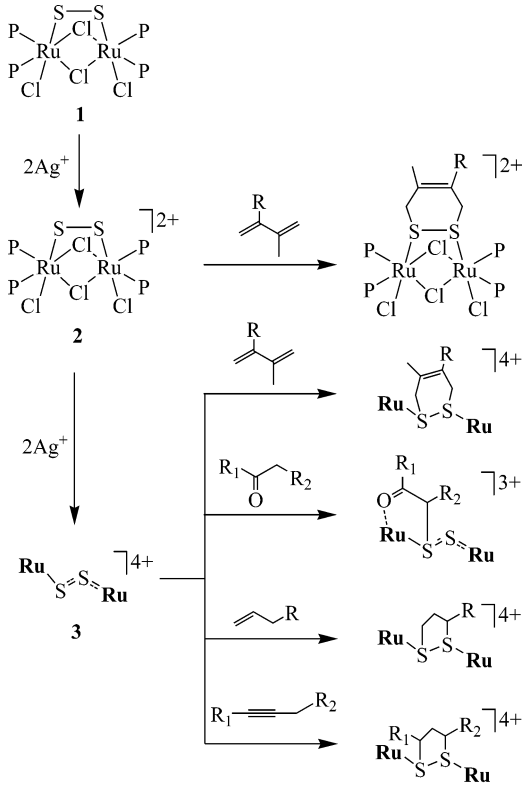

In our previous studies, although **3**, which has a trans $Ru^{III}SSRu^{III}$ core, is involved in a variety of C−H cleavage and C−S bond forming reactions, **3** is often reduced to the trans $Ru^{II}SSRu^{III}$ complex $[\{Ru(P(OCH_3)_3)_2(CH_3CN)_3\}_2(\mu\text{-}S_2)]^{3+}$ at the same time as C−S bond formation, and the $Ru^{II}SSRu^{III}$ complex is not reactive toward unsaturated substrates. The reactivity of the disulfide RuSSRu complex is affected by many factors, such as the cis−trans of the core structure, the steric congestion around the RuSSRu core, and the nature of the ligands, especially those trans to the disulfide. To study these effects, we synthesized *cis*-$Ru^{III}SSRu^{III}$ complexes, which have a dicyanido-bridging ligand coordinated trans to the disulfido ligand. The dicyanido-bridged complexes are very reactive toward olefins, and two different alkyl additions occurred on the two sulfur atoms of the same disulfido ligand.

Experimental Section

All of the reactions were carried out under an Ar or N_2 atmosphere using standard Schlenk line technique. Dry and oxygen-free solvents were purchased from Kanto Chemical Co. Acetonitrile-d_3 was dried over CaH_2 and distilled by trap-to-trap distillation prior to use. The reagents were purchased and used without further purification. **1-Cl** was prepared according to the procedure as described in the literature, whereas **1-Br** was converted from **1-Cl** by reacting with Me_3SiBr.[13] Through the Experimental Section and the Results and Discussion section, the same compound numbering is used for both chloride and bromide congeners. The NMR spectra were recorded on JEOL Lambda-270, Lambda-500, and Avance-400 spectrometers. The chemical shift (δ) is referenced to TMS for ^1H NMR and 85% H_3PO_4 for ^{31}P NMR. Elemental analysis was performed using a Perkin-Elmer PE2000 microanalyzer at Material Characterization Central Laboratory in Waseda University. Electrospray ionization mass spectra were recorded using a Finnigan LCQ DECA spectrometer. The ESI source was operated at 4.25 kV, the capillary heater was set to 453 K, and the experiments were performed in positive ion mode.

Synthesis of $[\{Ru(P(OCH_3)_3)_2\}_2(\mu\text{-}S_2)(\mu\text{-}X)_2\{\mu\text{-}m\text{-}C_6H_4(CH_2CN)_2\}](CF_3SO_3)_2$ (4) (X = Cl, Br). To a CH_3OH (1.0 mL) solution of $[\{Ru(P(OCH_3)_3)_2Cl\}_2(\mu\text{-}S_2)(\mu\text{-}Cl)_2]$ (**1-Cl**) (90.4 mg, 0.10 mmol) was added $AgCF_3SO_3$ (51.2 mg, 0.20 mmol), and the mixture was stirred at ambient temperature for 12 h. The solvent was removed by reduced pressure, and the residue was washed with Et_2O (10 mL) and dried in vacuo. The residue was dissolved in CH_2Cl_2, and *m*-xylylenedicyanide was added. The solution was stirred at ambient temperature for 12 h. Volatiles were removed under reduced pressure, and the remaining solid was washed three times with DME (10 mL) and dried in vacuo. The residue was recrystallized from CH_2Cl_2/DME to give green crystals of $[\{Ru(P(OCH_3)_3)_2\}_2(\mu\text{-}S_2)(\mu\text{-}Cl)_2\{\mu\text{-}m\text{-}C_6H_4(CH_2CN)_2\}](CF_3SO_3)_2$ (**4-Cl**). Yield: 61%. Anal. Calcd for $C_{24}H_{44}F_6N_2O_{18}P_4Ru_2S_4Cl_2$: C, 22.38; H, 3.44; N, 2.18. Found: C, 22.47; H, 3.45; N, 2.10. ^1H NMR ($CDCl_3$, 270 MHz, 233.3 K, δ): 3.80−3.90 (br, 36H, $P(OCH_3)_3$), 4.75 (br, 4H, CH_2CN), 7.24−7.32 (m, 2H, C_6H_5), 7.35−7.43 (m, 1H, C_6H_5), 8.12 (s, 1H, C_6H_5). $^{31}P\{^1H\}$ NMR ($CDCl_3$, 109 MHz, 233.3 K, δ): 120.0 (s).

4-Br: $[\{Ru(P(OCH3)3)_2\}_2(\mu\text{-}S_2)(\mu\text{-}Br)_2\{\mu\text{-}m\text{-}C_6H_4(CH_2CN)_2\}](CF_3SO_3)_2$. Yield: 58%. Anal. Calcd for $C_{24}H_{44}F_6N_2O_{18}P_4Ru_2S_4Br_2$: C, 20.94; H, 3.22; N, 2.03. Found: C, 21.12; H, 3.26; N, 2.01. ^1H NMR ($CDCl_3$, 270 MHz, 243.3 K, δ): 3.80−3.90 (br, 36H, $P(OCH_3)_3$), 4.74 (br, 4H, CH_2CN), 7.25−7.37 (m, 2H, C_6H_5), 7.37−7.42 (m, 1H, C_6H_5), 8.28 (s, 1H, C_6H_5). $^{31}P\{^1H\}$ NMR ($CDCl_3$, 109 MHz, 243.3 K, δ): 121.0 (s).

Synthesis of $[\{Ru(P(OCH_3)_3)_2\}_2(\mu\text{-}S_2)(\mu\text{-}X)_2\{\mu\text{-}m\text{-}C_6H_4(CH_2CN)_2\}](CF_3SO_3)$ (5) (X = Cl, Br). To a CH_2Cl_2 (1.0 mL) solution of **4-Cl** (128.8 mg, 0.10 mmol) was added triphenylsilane (51.2 mg), and the mixture was stirred at ambient temperature for 3 days, followed by the removal of volatiles by reduced pressure. The residue was washed with Et_2O (10 mL) and dried in vacuo. The remaining solid was washed three times with Et_2O (10 mL) and dried in vacuo. The residue was recrystallized from CH_2Cl_2/Et_2O to give brown crystals of $[\{Ru(P(OCH_3)_3)_2\}_2(\mu\text{-}S_2)(\mu\text{-}Cl)_2\{\mu\text{-}m\text{-}C_6H_4(CH_2CN)_2\}](CF_3SO_3)$ (**5-Cl**). Yield: 61%. Anal. Calcd (%) for $C_{23}H_{44}F_3N_2O_{15}P_4Ru_2S_3Cl_2$: C, 24.26; H, 3.89; N, 2.46. Found: C, 24.91; H, 4.02; N, 2.08.

5-Br: Brown crystals of $[\{Ru(P(OCH_3)_3)_2\}_2(\mu\text{-}S_2)(\mu\text{-}Br)_2\{\mu\text{-}m\text{-}C_6H_4(CH_2CN)_2\}](CF_3SO_3)$ were isolated. Yield: 58%. Anal. Calcd (%) for $C_{23}H_{44}F_3N_2O_{15}P_4Ru_2S_3Br_2$: C, 22.50; H, 3.61; N, 2.28. Found: C, 22.87; H, 3.43; N, 2.09.

Synthesis of $[\{Ru(P(OCH_3)_3)_2\}_2(\mu\text{-}SCH_2C(CH_3){=}C(CH_3)CH_2S)(\mu\text{-}X)_2\{\mu\text{-}m\text{-}C_6H_4(CH_2CN)_2\}](CF_3SO_3)_2$ (6) (X = Cl, Br). To a CH_2Cl_2 (1.0 mL) solution of **4-Cl** (128.8 mg, 0.10 mmol) was added 2,3-dimethyl-1,3-butadiene (0.10 mL), and the mixture was stirred at ambient temperature for 3 h followed by the removal of volatiles in vacuo. The residue was washed with Et_2O (10 mL) and dried in vacuo. The residue was recrystallized from CH_2Cl_2/DME to give pale-green crystals of $[\{Ru(P(OCH_3)_3)_2\}_2(\mu\text{-}SCH_2C(CH_3){=}C(CH_3)CH_2S)(\mu\text{-}Cl)_2\{\mu\text{-}C_6H_4(CH_2CN)_2\}](CF_3SO_3)_2$ (**6-Cl**). Yield: 56%. Anal. Calcd (%) for $C_{30}H_{54}F_6N_2O_{18}P_4Ru_2S_4Cl_2$: C, 26.30; H, 3.97; N, 2.04. Found: C, 26.28; H, 3.87; N, 1.96. ^1H NMR (CD_3OD, 270 MHz, 233.3 K, δ): 1.92 (s, 6H, CCH_3), 3.41

(13) Ishizu, S.; Matsumoto, K. Unpublished results.

Table 1. Summary of Crystallographic Data

	4-Cl	**4-Br**	**5-Cl**	**5-Br**		**4-Cl**	**4-Br**	**5-Cl**	**5-Br**
formula	$C_{24}H_{44}Cl_2F_6N_2O_{18}P_4Ru_2S_4$	$C_{24}H_{44}Br_2F_6N_2O_{18}P_4Ru_2S_4$	$C_{23}H_{44}Br_2F_3N_2O_{15}P_4Ru_2S_3$	$C_{23}H_{44}Cl_2F_3N_2O_{15}P_4Ru_2S_3$	d_{calcd} (g·cm^{-3})	1.751	1.929	1.785	1.938
fw	1287.77	1376.69	1138.70	1227.62	μ (mm^{-1})	1.117	2.724	1.213	2.994
cryst syst	triclinic	triclinic	orthorhombic	triclinic	T (K)	293(2)	293(2)	293(2)	123(2)
No.	*P*1 (No. 2)	*P*1 (No. 2)	*Pca*2$_1$ (No. 29)	*P*1 (No. 2)	diffracto-meter	SMART 1000	SMART 1000	SMART 1000	SMART 1000
a (Å)	12.856(7)	12.960(2)	18.818(12)	12.2984(15)	abs corr	SADABS	SADABS	SADABS	SADABS
b (Å)	14.168(8)	13.624(2)	13.172(8)	13.0334(15)	reflns (total)	10 463	9985	7492	8951
c (Å)	14.389(8)	14.275(2)	17.090(10)	13.5373(16)	reflns ($F_o^2 > 2\sigma(F_o^2)$)	4684	8386	5870	7280
α (deg)	105.010(10)	104.220(3)		82.017(2)	params	491	491	459	459
β (deg)	93.850(10)	94.368(3)		78.268(2)	R1[a]	0.0867	0.0636	0.0541	0.0437
γ (deg)	103.128(10)	101.795(3)		89.181(2)	wR2[b]	0.1989	0.1796	0.1342	0.1086
V (Å^3)	2443(2)	2370.2(7)	4236(4)	2103.8(4)	GOF[c]	1.025	1.078	1.017	1.024
Z	2	2	4	2					

	6-Cl	**6-Br**	**7**	**8**		**6-Cl**	**6-Br**	**7**	**8**
formula	$C_{30}H_{54}Cl_2F_6N_2O_{18}P_4Ru_2S_4$	$C_{30}H_{54}Br_2F_6N_2O_{18}P_4Ru_2S_4$	$C_{28}H_{53}Cl_2F_3N_2O_{15}P_4Ru_2S_3$	$C_{30}H_{56}Cl_2F_6N_2O_{18}P_4Ru_2S_4$	d_{calcd} (g·cm^{-3})	1.747	1.938	1.724	1.748
fw	1369.91	1376.69	1207.82	1371.93	μ (mm^{-1})	1.053	2.588	1.110	1.052
cryst syst	triclinic	triclinic	triclinic	triclinic	T (K)	293(2)	123(2)	120(2)	120(2)
No.	*P*1 (No. 2)	*P*1 (No. 2)	*P*1 (No. 2)	*P*1 (No. 2)	diffracto-meter	SMART 1000	SMART 1000	SMART 1000	SMART 1000
a (Å)	8.982(6)	9.367(4)	11.906(5)	12.2103(18)	abs corr	SADABS	SADABS	SADABS	SADABS
b (Å)	13.158(8)	11.691(5)	13.125(6)	13.232(2)	reflns (total)	11 268	10 468	9857	11 153
c (Å)	23.180(14)	23.899(11)	15.181(6)	16.283(2)	reflns ($F_o^2 > 2\sigma(F_o^2)$)	7179	7900	6883	8657
α (deg)	104.245(12)	102.601(8)	80.023(7)	103.258(12)	params	547	547	505	547
β (deg)	97.383(11)	99.426(9)	86.096(8)	94.601(12)	R1[a]	0.0704	0.0754	0.0727	0.0626
γ (deg)	96.312(12)	94.774(9)	85.906(8)	95.267(14)	wR2[b]	0.1839	0.1897	0.1987	0.1570
V (Å^3)	2605(3)	2500.4(19)	2326.7(17)	2607(3)	GOF[c]	1.067	1.070	1.047	1.046
Z	2	2	2	2					

	9	**10**	**11**	**12**		**9**	**10**	**11**	**12**
formula	$C_{29}H_{55}Cl_2F_3N_2O_{15}P_4Ru_2S_3$	$C_{31}H_{57}Cl_2F_6N_2O_{18}P_4Ru_2S_4$	$C_{28}H_{50}Cl_2F_6N_2O_{18}P_4Ru_2S_4$	$C_{27}H_{51}Cl_2F_3N_2O_{16}P_4Ru_2S_3$	d_{calcd} (g·cm^{-3})	1.687	1.728	1.826	1.755
fw	1221.85	1384.95	1341.86	1209.80	μ (mm^{-1})	1.074	1.031	1.122	1.130
cryst syst	triclinic	triclinic	triclinic	triclinic	T (K)	120(2)	120(2)	120(2)	120(2)
No.	*P*1 (No. 2)	*P*1 (No. 2)	*P*1 (No. 2)	*P*1 (No. 2)	diffracto-meter	SMART 1000	SMART 1000	SMART 1000	SMART 1000
a (Å)	12.2103(18)	8.915(9)	8.8148(12)	11.7128(15)	abs corr	SADABS	SADABS	SADABS	SADABS
b (Å)	13.232(2)	12.413(12)	12.4503(17)	13.0959(17)	reflns (total)	10 249	11 315	10 331	9769
c (Å)	16.283(2)	24.95(2)	23.230(3)	15.2169(19)	reflns ($F_o^2 > 2\sigma(F_o^2)$)	8080	6672	8711	5605
α (deg)	66.210(2)	103.957(18)	102.872(3)	80.371(3)	params	514	574	527	505
β (deg)	88.096(3)	91.684(18)	98.455(2)	85.484(3)	R1[a]	0.0955	0.0753	0.0448	0.0825
γ (deg)	88.014(3)	95.768(16)	94.801(2)	85.406(2)	wR2[b]	0.2467	0.1860	0.1122	0.2167
V (Å^3)	2405.3(6)	2662(4)	2440.3(6)	2288.8(5)	GOF[c]	1.011	1.028	1.047	1.029
Z	2	2	2	2					

[a] $R1 = \sum|F_o - F_c|/\sum|F_o|$ for reflections $F_o^2 > 2\sigma(F_o^2)$. [b] $wR2 = [\sum w(F_o^2 - F_c^2)^2/\sum w(F_o^2)^2]^{1/2}$. [c] $GOF = [\sum w(F_o^2 - F_c^2)^2/\sum(n-p)]^{1/2}$.

(d, J = 13.5 Hz, 2H, SC*H*H′), 3.81 (vt, $^3J_{PH}$ = 14.5 Hz, 36H, P(OC*H*$_3$)$_3$), 3.98 (d, J = 8.6 Hz, 2H, SCH*H*′), 4.56 (s, 4H, C*H*$_2$-CN), 7.24−7.32 (m, 2H, C$_6$*H*$_5$), 7.35−7.39 (m, 1H, C$_6$*H*$_5$), 7.88 (s, 1H, C$_6$*H*$_5$). ^{31}P{^{1}H} NMR (CD$_3$OD, 109 MHz, 233.3 K, δ): 128 (m), 130.8 (m).

6-Br: Yield: 47%. Anal. Calcd for $C_{30}H_{54}F_6N_2O_{18}P_4Ru_2S_4Br_2$: C, 24.70; H, 3.73; N, 1.92. Found: C, 24.65; H, 3.55; N, 1.88. ^{1}H NMR (CD$_3$OD, 270 MHz, 253.3 K, δ): 1.96 (s, 6H, CC*H*$_3$), 3.52 (d, J = 13.2 Hz, 2H, SC*H*H′), 3.87 (vt, $^3J_{PH}$ = 9.7 Hz, 36H, P(OC*H*$_3$)$_3$), 4.21 (d, J = 14.0 Hz, 2H, SCH*H*′), 4.70 (s, 4H, C*H*$_2$-CN), 7.28−7.32 (m, 2H, C$_6$*H*$_5$), 7.43−7.50 (m, 1H, C$_6$*H*$_5$), 8.15 (s, 1H, C$_6$*H*$_5$). ^{31}P{^{1}H} NMR (CD$_3$OD, 109 MHz, 253.3 K, δ): 130.5 (m), 132.7 (m).

Reactions with Terminal Alkenes. To a CH$_3$OH (1.0 mL) solution of complex **4-Cl** (128.8 mg, 0.10 mmol) was added

Scheme 2. Synthesis of **4**

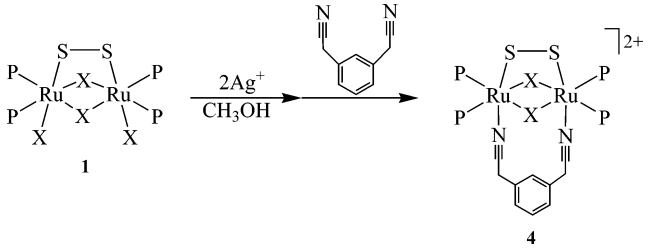

1 4

1-pentene (0.10 mL), and the solution was stirred at ambient temperature for 1 d, followed by the removal of volatiles in vacuo. The residue was washed with Et$_2$O (10 mL) and dried in vacuo. The residue was then recrystallized from CH$_3$OH/Et$_2$O to give green crystals of [{Ru(P(OCH$_3$)$_3$)$_2$}$_2$(μ-SCH$_2$CH═CHCH$_2$CH$_3$S)(μ-Cl)$_2$-

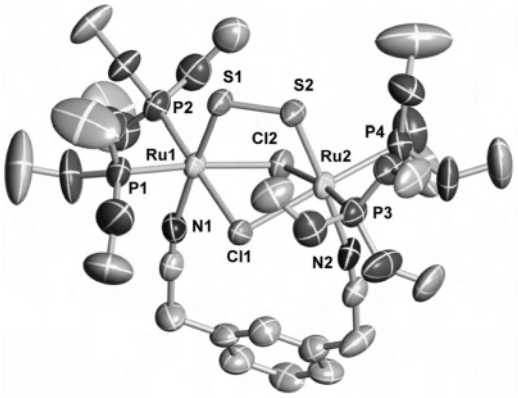

Figure 1. ORTEP diagram of the cation of **4-Cl** with 50% thermal ellipsoids.

Table 2. Selected Bond Distances (anstroms), Angles (deg), and Torsion Angles (deg) of **4** and **5**

	4-Cl	4-Br	5-Cl	5-Br
		Bond Distances		
Ru1−P1	2.260(4)	2.2603(14)	2.206(3)	2.2220(14)
Ru1−P2	2.257(3)	2.2570(14)	2.226(2)	2.2233(14)
Ru2−P3	2.265(4)	2.2674(14)	2.218(3)	2.2172(14)
Ru2−P4	2.257(4)	2.2564(15)	2.218(2)	2.2298(13)
Ru1−S1	2.198(3)	2.2022(13)	2.292(3)	2.3053(13)
Ru2−S2	2.198(3)	2.2103(14)	2.286(2)	2.3055(12)
Ru1−X1	2.478(3)	2.5911(7)	2.491(2)	2.6400(7)
Ru1−X2	2.501(3)	2.6223(7)	2.504(2)	2.6140(6)
Ru2−X1	2.480(3)	2.5965(8)	2.495(2)	2.6342(6)
Ru2−X2	2.514(3)	2.6289(8)	2.509(2)	2.6101(6)
Ru1−N1	2.086(10)	2.094(5)	2.063(7)	2.068(4)
Ru2−N2	2.081(11)	2.083(5)	2.086(7)	2.070(4)
S1−S2	1.974(4)	1.9726(19)	1.995(3)	2.0131(18)
		Bond Angles		
S2−S1−Ru1	110.99(16)	111.83(7)	110.01(11)	111.35(6)
S1−S2−Ru2	110.19(15)	111.59(7)	109.01(11)	110.95(6)
S1−Ru1−N1	176.4(3)	175.20(13)	175.99(19)	173.37(12)
S2−Ru2−N2	176.2(3)	175.37(12)	173.7(2)	175.19(12)
Ru1−X1−Ru2	90.50(10)	88.07(2)	90.89(8)	88.518(19)
Ru1−X2−Ru2	89.18(10)	86.732(19)	90.28(9)	89.59(2)
X1−Ru1−X2	80.39(10)	82.56(2)	80.53(7)	82.71(2)
X1−Ru2−X2	80.11(10)	82.33(2)	80.36(7)	82.90(2)
		Torsion Angles[a]		
Ru1−S1−S2−Ru2	1.6(2)	2.12(9)	12.16(15)	4.71(9)

[a] Reported without the sign.

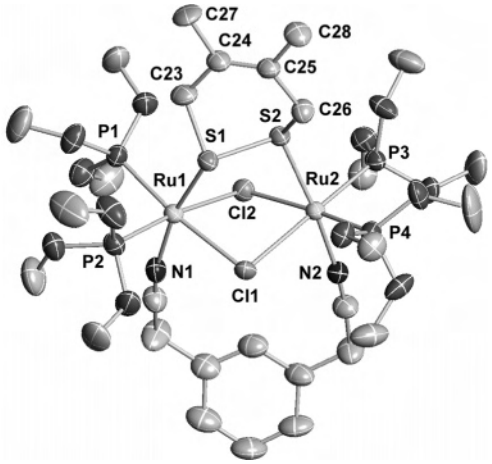

Figure 2. ORTEP diagram of the cation of **6-Cl** with 50% thermal ellipsoids.

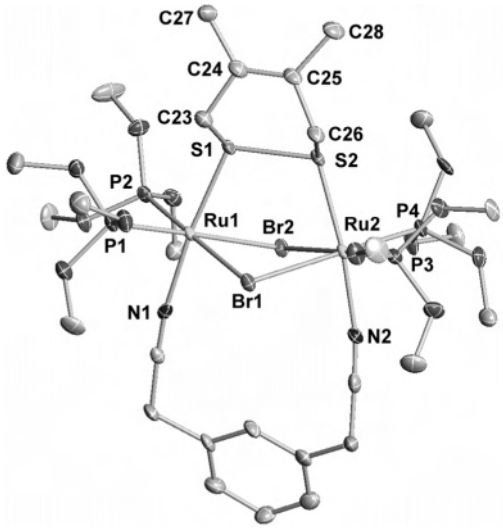

Figure 3. ORTEP diagram of the cation of **6-Br** with 50% thermal ellipsoids.

$\{\mu$-*m*-$C_6H_4(CH_2CN)_2\}]$ $(CF_3SO_3)_2$ (**7**), pale-green crystals of $[\{Ru(P(OCH_3)_3)_2\}_2(\mu$-$SCH_2CH{=}CHCH_2CH_3SCH_3)(\mu$-$Cl)_2\{\mu$-*m*-$C_6H_4(CH_2CN)_2\}](CF_3SO_3)_2$ (**8**), brown crystals of **5-Cl**, and unidentified compounds.

7: Anal. Calcd for $C_{28}H_{53}F_6N_2O_{15}P_4Ru_2S_3Cl_2$: C, 27.84; H, 4.42; N, 2.32. Found: C, 27.57; H, 4.45; N, 2.25. ^{1}H NMR (CD_3OD, 500 MHz, 233.3 K, δ): 1.04 (tr, J = 7.4 Hz, 3H, CH_2CH_3), 2.10 (m, 2H, $CH_2CH_2CH_3$), 3.24 (m, 1H, SC*H*H′), 3.79 (vt, $^3J_{PH}$ = 11.3 Hz, 36H, $P(OCH_3)_3$), 3.90 (m, 1H, SCH*H*′), 4.56 (s, 2H, CH_2CN), 4.46 (s, 2H, CH_2CN), 5.68−5.80 (m, 2H, $CH_2CH{=}CHCH_2$), 7.25 (m, 2H, C_6H_5), 7.40 (m, 1H, C_6H_5), 8.18 (s, 1H, C_6H_5). $^{31}P\{^1H\}$ NMR (CD_3CN, 109 MHz, r.t., δ): 125.4 (m), 135.5 (m), 138.8 (s).

8: Anal. Calcd for $C_{30}H_{56}F_6N_2O_{18}P_4Ru_2S_4Cl_2$: C, 26.26; H, 4.11; N, 2.04. Found: C, 24.50; H, 3.83; N, 2.36. ^{1}H NMR (CD_3OD, 500 MHz, r.t., δ): 1.08 (tr, J = 7.5 Hz, 3H, CH_2CH_3), 2.18 (m, 2H, $CH_2CH_2CH_3$), 3.52 (m, 1H, SC*H*H′), 3.79 (vt, $^3J_{PH}$ = 11.3 Hz, 36H, $P(OCH_3)_3$), 4.16 (m, 1H, SCH*H*′), 4.65 (s, 4H, CH_2CN), 5.76 (m, 1H, $SCH_2CH{=}CHCH_2$), 6.00 (m, 1H, $SCH_2CH{=}CHCH_2$), 7.30 (m, 2H, C_6H_5), 7.45 (m, 1H, C_6H_5), 8.08 (s, 1H, C_6H_5). $^{31}P\{^1H\}$ NMR (CD_3OD, 109 MHz, r.t., δ): 125.4 (m).

4-Cl (128.8 mg, 0.10 mmol) and 1-hexene in CH_3OH (1.0 mL) afforded green crystals of $[\{Ru(P(OCH_3)_3)_2\}_2(\mu$-$SCH_2CH{=}CH(CH_2)_2CH_3S)(\mu$-$Cl)_2\{\mu$-*m*-$C_6H_4(CH_2CN)_2\}]$ $(CF_3SO_3)_2$ (**9**), $[\{Ru(P(OCH_3)_3)_2\}_2(\mu$-$SCH_2CH{=}CH(CH_2)_2CH_3SCH_3)(\mu$-$Cl)_2$ $\{\mu$-*m*-$C_6H_4(CH_2CN)_2\}](CF_3SO_3)_2$ (**10**) as pale-green crystals, **5-Cl** as brown crystals, and unidentified compounds.

9: Anal. Calcd for $C_{29}H_{55}F_3N_4O_{15}P_4Ru_2S_3Cl_2$: C, 26.86; H, 4.22; N, 2.02. Found: C, 26.54; H, 4.16; N, 1.81. ^{1}H NMR (CD_3OD, 500 MHz, r.t., δ): 1.04 (tr, J = 7.4 Hz, 3H, CH_2CH_3), 2.10 (m, 2H, $CH_2CH_2CH_3$), 3.24 (m, 1H, SC*H*H′), 3.79 (vt, $^3J_{PH}$ = 11.3 Hz, 36H, $P(OCH_3)_3$), 3.90 (m, 1H, SCH*H*′), 5.68−5.80 (m, 2H, $CH_2CH{=}CHCH_2$), 7.25 (m, 2H, C_6H_5), 7.40 (m, 1H, C_6H_5), 8.18 (s, 1H, C_6H_5). $^{31}P\{^1H\}$ NMR (CD_3CN, 109 MHz, r.t., δ): 125.4 (m).

10: Anal. Calcd for $C_{31}H_{58}F_6N_4O_{18}P_4Ru_2S_4Cl_2$: C, 28.51; H, 4.54; N, 2.29. Found: C, 28.83; H, 4.73; N, 2.03. ^{1}H NMR (CD_3OD, 500 MHz, r.t., δ): 0.88 (tr, J = 7.1 Hz, 3H, CH_2CH_3), 1.40 (m, 2H, $CH_2CH_2CH_3$), 2.07 (m, 2H, $CHCH_2CH_2$), 3.42 (m, 1H, SC*H*H′), 3.81 (vt, $^3J_{PH}$ = 11.3 Hz, 36H, $P(OCH_3)_3$), 4.10 (m, 1H, SCH*H*′), 4.52 (m, 4H, CH_2CN), 5.59 (m, 1H, $SCH_2CH{=}CHCH_2$), 5.79 (m, 1H, $SCH_2CH{=}CHCH_2$), 7.30 (m, 2H, C_6H_5), 7.45 (m,

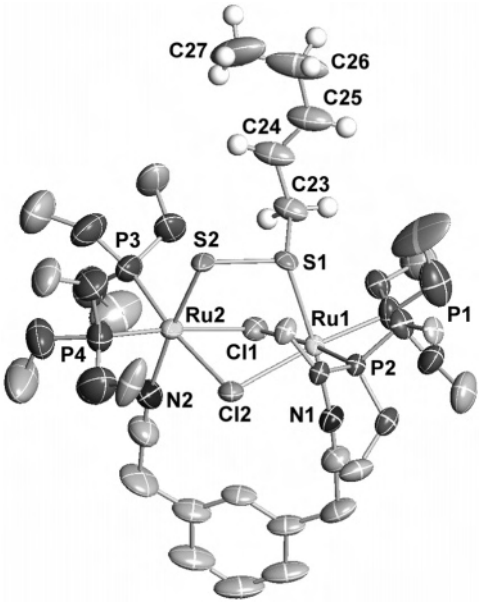

Figure 4. ORTEP diagram of **7** with 50% thermal ellipsoids.

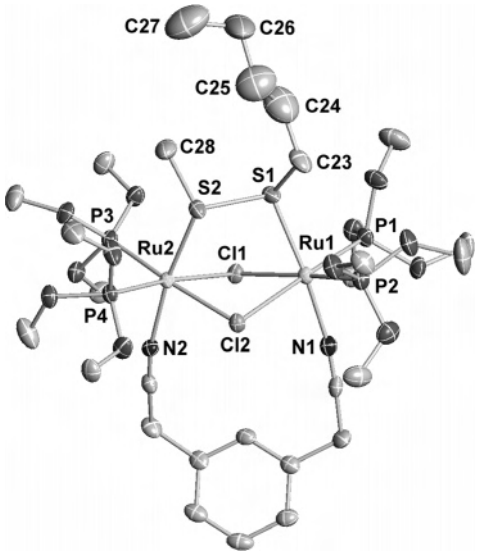

Figure 5. ORTEP diagram of **8** with 50% thermal ellipsoids.

1H, C_6H_5), 8.08 (s, 1H, C_6H_5). $^{31}P\{^1H\}$ NMR (CD_3OD, 162 MHz, 233.3 K, δ): 128.5 (m), 132 (m).

Reaction of Internal Alkenes. To a CH_3OH (1.0 mL) solution of **4-Cl** (128.8 mg, 0.10 mmol) was added 2-pentene (21.6 μL), and the mixture was stirred at ambient temperature for 1 d, followed by the removal of volatiles in vacuo. The residue was washed with Et_2O (10 mL), dried in vacuo, and recrystallized from CH_3OH/Et_2O to give complexes **8** and **5-Cl** and an unidentified compound.

Similarly, the reaction of 2-hexene (24.8 μL) and **4-Cl** (128.8 mg, 0.10 mmol) in CH_3OH (1.0 mL) afforded complexes **10**, **5-Cl**, and unidentified compounds.

Synthesis of [{Ru(P(OCH$_3$)$_3$)$_2$}$_2$(μ-SCH$_2$CH═CHCH$_2$S)(μ-Cl)$_2${μ-*m*-C$_6$H$_4$(CH$_2$CN)$_2$}] (CF$_3$SO$_3$)$_2$ (11). To a CH_3OH (1.0 mL) solution of **4-Cl** (128.8 mg, 0.10 mmol) was added 4-bromo-1-butene (0.10 mL), and the solution stirred at ambient temperature for 1 d, followed by the removal of volatiles in vacuo. The residue was washed with Et_2O (10 mL) and dried in vacuo. The residue was recrystallized from CH_3OH/Et_2O to give pale-green crystals of [{Ru(P(OCH$_3$)$_3$)$_2$}$_2$(μ-SCH$_2$CH═CHCH$_2$S)(μ-Cl)$_2${μ-*m*-C$_6$H$_4$(CH$_2$CN)$_2$}](CF$_3$SO$_3$)$_2$ (**11**). Yield: 77%. Anal. Calcd. for $C_{28}H_{50}F_6N_4O_{18}P_4Ru_2S_4Cl_2$: C, 25.06; H, 3.76; N, 2.09. Found: C, 24.87; H, 3.56; N, 2.10. ^1H NMR (CD_3OD, 270 MHz, 253.3K): δ 3.52 (br, 2H, CH_2CN), 3.85 (br, 18H, P(OCH_3)$_3$), 3.89 (br, 18H, P(OCH_3)$_3$), 4.23 (br, 2H, CH_2CN), 4.65 (br, 4H, CH_2CN), 6.18 (br, 2H, CH═CH), 7.28 (m, 2H, C_6H_5), 7.44 (m, 1H, C_6H_5), 8.05 (s, 1H, C_6H_5). $^{31}P\{^1H\}$ NMR (CD_3OD, 109 MHz, 253.3K): δ 130.0 (m).

Scheme 3. Reduction of **4**

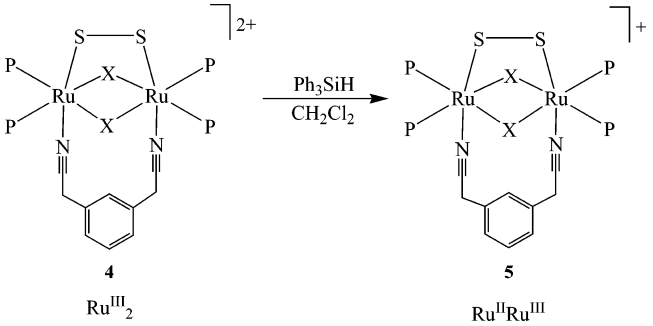

Scheme 4. Reaction of **4** with Diene

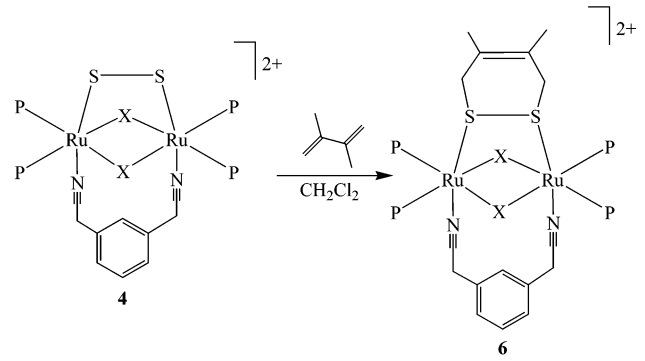

Reaction with 3-Butene-1-ol. To a CH_3OH (1.0 mL) solution of **4-Cl** (128.8 mg, 0.10 mmol) was added 3-butene-1-ol (0.10 mL), and the mixture was stirred at ambient temperature for 1 d, followed by the removal of volatiles in vacuo. The residue was washed with Et_2O (10 mL) and dried in vacuo. The residue was recrystallized from CH_3OH/Et_2O to give **11** as green crystals and [{Ru(P(OCH$_3$)$_3$)$_2$}$_2$(μ-SCH$_2$CH═CHCH$_2$OHS)(μ-Cl)$_2${μ-*m*-C$_6$H$_4$(CH$_2$CN)$_2$}] (CF$_3$SO$_3$) (**12**) as pale-green crystals. Anal. Calcd (%) for $C_{27}H_{51}F_3N_2O_{16}P_4Ru_2S_3Cl_2$: C, 26.80; H, 4.25; N, 2.32. Found: C, 26.11; H, 3.75; N, 2.00. ^1H NMR ($CDCl_3$, 500 MHz, 253.3 K, δ): 3.25 (m, 1H, SCHH′), 3.76 (vt, $^3J_{PH}$ = 8.4 Hz, 36H, P(OCH_3)$_3$), 3.96 (m, 1H, SCHH′), 4.14 (d, J = 4.0 Hz, 2H, CH$_2$CH_2OH), 5.84−5.96 (m, 2H, CH$_2$CH═CHCH$_2$), 7.13 (m, 2H, C_6H_5), 7.32 (m, 1H, C_6H_5), 8.10 (s, 1H, C_6H_5). $^{31}P\{^1H\}$ NMR ($CDCl_3$, 500 MHz, 253.3 K, δ): 137.3 (m), 140.0 (m).

X-ray Diffraction Study. The diffraction data of **4**−**12** were collected using a Bruker CCD SMART 1000 area detector diffractometer with graphite-monochromated Mo Kα irradiation (λ = 0.71073 Å). The intensities of the reflections were integrated by the SAINT program. An absorption correction was applied for the collected data using SADABS software. Structure solutions were performed using a SHELXTL program package. Details of the crystallographic data are summarized in Table 1. All of the non-hydrogen atoms of the cations were refined anisotropically. All of the hydrogen atoms were generated and refined in ideal positions, and the positions of the methyl hydrogen atoms were refined with HFIX 137 instruction of the SHELXTL program. The hydrocarbon moiety on the disulfido ligand in **10** looks like a C_7S_2 nine-membered ring because of the disorder of the alkenyl chain on both

Scheme 5. C−S Bond Formation in **4**

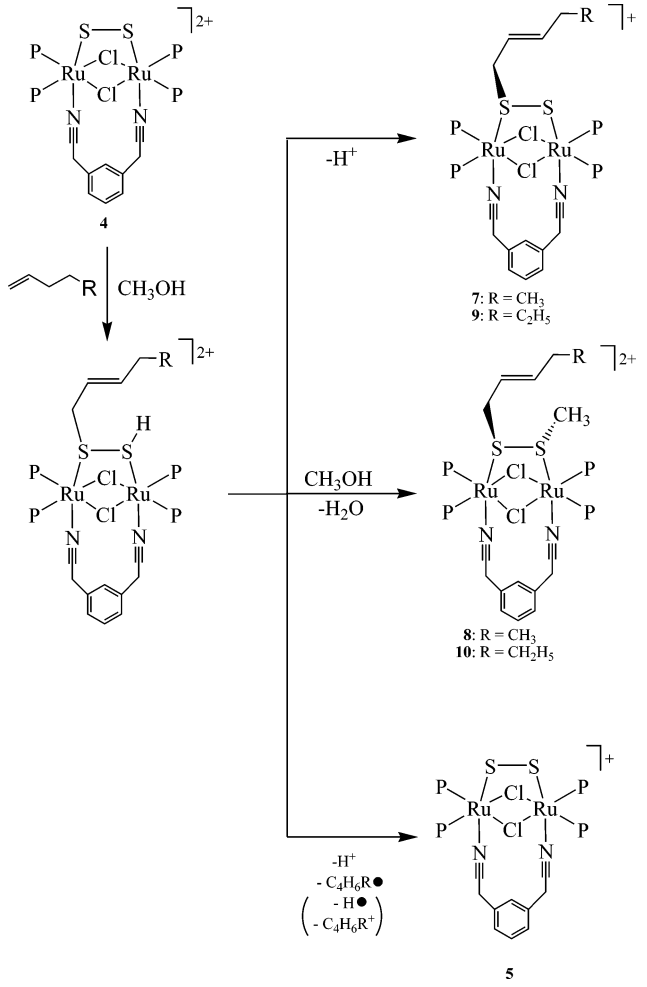

sulfur atoms. Actually, β- and γ-carbons are located at two positions with almost equivalent occupancies.

Results and Discussion

Reaction of $[\{Ru(P(OCH_3)_3)_2X\}_2(\mu\text{-}S_2)(\mu\text{-}X)_2]$ (**1**) with 2 equiv of $AgCF_3SO_3$ in CH_3OH, followed by reaction with *m*-xylylenedicyanide in CH_2Cl_2, afforded $[\{Ru(P(OCH_3)_3)_2\}_2(\mu\text{-}S_2)(\mu\text{-}X)_2\{\mu\text{-}C_6H_4(CH_2CN)_2\}](CF_3SO_3)_2$ (**4**, X = Cl, 61%; X = Br, 58%) (Scheme 2).

The structure of **4** with counterions was determined by single-crystal X-ray analysis. An ORTEP of the cation of **4-Cl** is shown in Figure 1, and selected bond distances and angles are listed in Table 2.

In the cation, the two $Ru(P(OCH_3)_3)_2$ moieties are bridged by two halide ions, one disulfido ligand, and a *m*-xylylenedicyanide ligand. Because the phenyl ring of the dicyanide ligand in **4** and the other complexes (Figures 1−5) crystallizes in different orientations, it is thought that in solution the benzene ring of the *m*-xylylenedicyanide ligand easily moves to either side of the RuSSRu plane at room temperature or dissociates and reassociates. The ^{1}H NMR spectrum of **4** showed a very broad signal at r.t.; however, the methylene signals of the *m*-xylylenedicyanido ligand became sharp below 0 °C. In addition to reorientation of the phenyl rings, *m*-xylylendicyanide is easily replaced by coordinating

Scheme 6. Proposed Mechanism for C−S Bond Formation in **3**

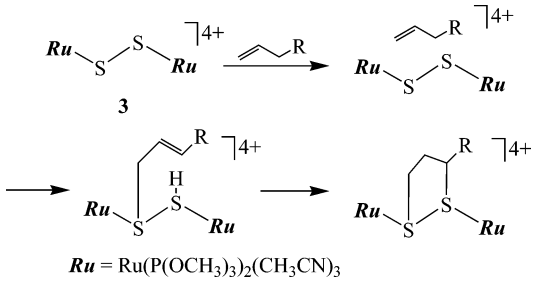

solvents, on the basis of the ^{1}H NMR spectrum in CD_3CN (Supporting Information). Thus, flexibility of the dicyanide ligand may be related to the unexpectedly weak coordination to the two Ru atoms.

The reaction of **4** with triphenylsilane gave the reduced complex$[\{Ru(P(OCH_3)_3)_2\}_2(\mu\text{-}S_2)(\mu\text{-}X)_2\{\mu\text{-}C_6H_4(CH_2CN)_2\}](CF_3SO_3)$ (**5**), in which the Ru ions are mixed valence Ru^{II}/Ru^{III} (Scheme 3). **5** also formed in several other reactions, described later. **5** is inactive toward olefins. However, because **5** formed during the reaction, it is clear that a redox reaction occurred at the same time as the C−S bond formation, which gives some insight into the reaction mechanism.

4 reacts with 2,3-dimethyl-1,3-butadiene in CH_2Cl_2 to afford $[\{Ru(P(OCH_3)_3)_2\}_2(\mu\text{-}SCH_2C(CH_3)=C(CH_3)CH_2S)(\mu\text{-}Cl)_2\{\mu\text{-}C_6H_4(CH_2CN)_2\}](CF_3SO_3)_2$ (**6**, X = Cl, 56%; X = Br, 47%), which is formally a [4 + 2] cycloaddition reaction product similar to those previously reported for **2** and **3** with a conjugated diene (Scheme 4).[8] The structures of **6-Cl** and **6-Br** are shown in Figures 2 and 3, respectively.

Cycloaddition may occur because of the structural stability of the product and is considered as a typical reaction of the disulfido ligand in our dinuclear Ru^{III} complexes.[14] The C_4S_2 six-membered ring is frequently formed through other different processes, as described later. Although **6** is stable, the molecule is flexible rather than rigid, and in solution, **6** also showed fluxional behavior. Temperature dependent ^{1}H and $^{31}P\{^1H\}$ NMR spectroscopy showed spectral changes upon changing the temperature from r.t. to 253 K (Supporting Information, ^{31}P NMR spectra of **9** at r.t. and 253 K). There are two possible explanations for the observed spectra: (1) the phosphites rapidly exchange, causing an averaging of the ^{31}P NMR peaks, and (2) the phenyl moiety in the dicyanide ligand moves back and forth with respect to the RuSSRu plane, as mentioned previously. For steric reasons and on the basis of the X-ray structures of the complexes, it is thought that the latter explanation is more plausible.

There are two possible mechanisms for this reaction: (1) a concerted mechanism in which bond cleavage and bond formation happen simultaneously and (2) a stepwise mechanism. However, the stepwise formation of the two C−S bonds cannot be ruled out, especially in reactions involving sulfur. Ionic or radical interactions between the terminal methylene carbon and the second S atom of the disulfido-bridging ligand may occur to form a stable six-membered ring after the first C−S bond is formed. Whichever the

(14) Sugiyama, H.; Watanabe, T.; Matsumoto, K. *Chem. Lett.* **2001**, 306−307.

Scheme 7. Proposed Mechanism for the Reaction of **4** with Internal Alkenes

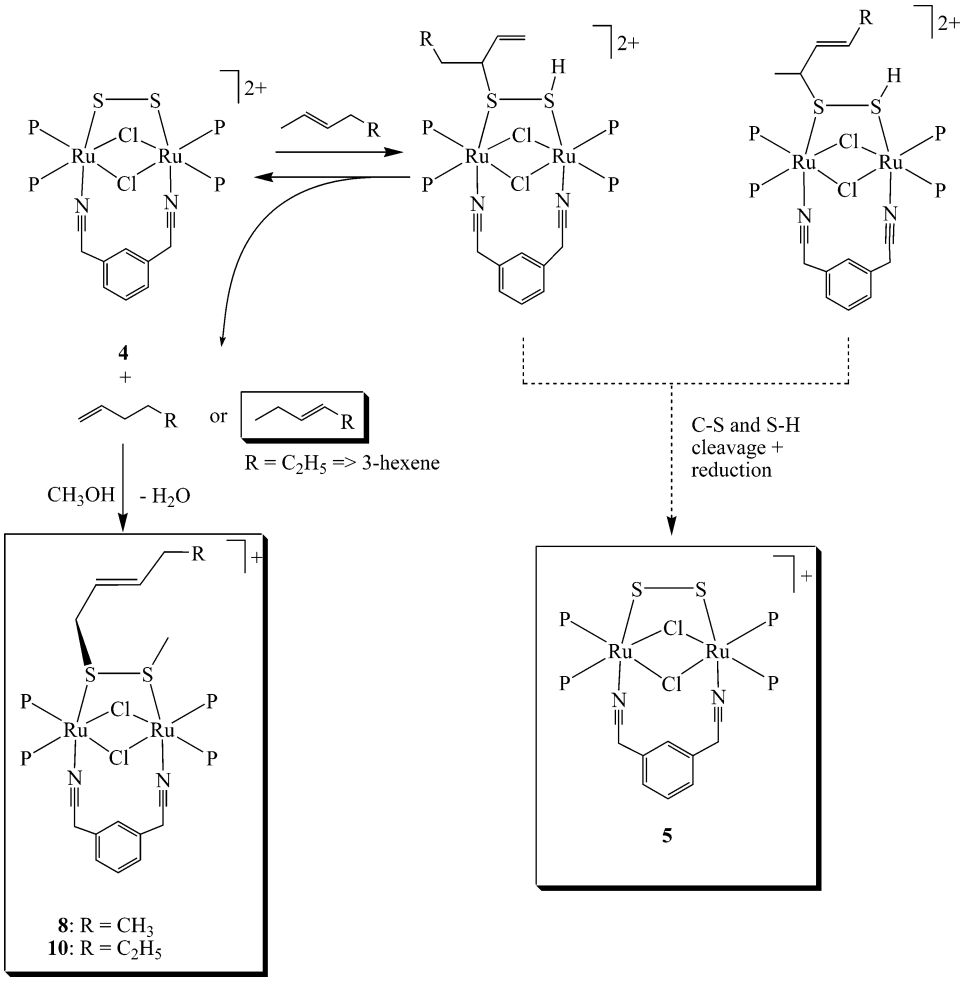

mechanism may be, the reactivity of the disulfido ligand observed with **2** toward dienes is maintained in the dicyanide-bridged **4**, and therefore, the reactivity of **4** was studied further.

The reaction of **4** with 1-pentene gave reduced **5** and two substrate-attached complexes (**7** and **8**) (Scheme 5). The structures of **7** and **8** are in Figures 4 and 5, respectively.

The overall charge of the ruthenium dimer species changed from 2+ to 1+ because of the release of a proton. The changes in the orbital hybridization of the carbon atoms and in the bond orders make this reaction seem similar to an ene-reaction.[15] The other product **8** that contains a C_5 chain has a methyl group on the other sulfur atom of the disulfido bridge. The solvent CH_3OH is thought to be the source of the CH_3 group of **8**, which was confirmed by carrying out the reaction in CD_3OD. In the ESI-MS spectrum of **8**-d_3, the peak envelope is clearly shifted 3 amu compared to that of **8**, and it has the expected isotope pattern. The formation of **8**, therefore, involves the addition of 1-pentene and CH_3OH along with the elimination of H_2O. This is an unexpected and unprecedented reaction. Unlike the [4 + 2] addition reactions with conjugated dienes,[8] the reaction with alkenes involves a C−H bond cleavage step, which also occurs in the various reactions of **3** (Scheme 1). In these reactions, a hydrogen atom of the alkene is thought to have shifted to its final position in the product via the sulfur atom (Scheme 6).

However, there is no direct evidence. Hydrosulfido ligands are known in several other transition-metal complexes,[16−34] and hydrogen addition from these complexes to an unsatur-

(15) Davies, A. G.; Kinart, W. J. *J. Chem. Soc., Perkin Trans.* **1993**, 2281.

(16) Rakowski DuBois, M.; VanDerveer, M. C.; DuBois, D. L.; Haltiwanger, D. L.; Miller, W. K. *J. Am. Chem. Soc.* **1980**, *102*, 7456−7461.
(17) Rakowski DuBois, M.; DuBois, D. L.; VanDerveer, M. C.; Haltiwanger, R. C. *Inorg. Chem.* **1981**, *20*, 3064−3071.
(18) Ruffing, C. J.; Rauchfuss, T. B. *Organometallics* **1985**, *4*, 524−528.
(19) Kuwata, S.; Hidai, M. *Coord. Chem. Rev.* **2001**, *213*, 211−305.
(20) Kabashima, S.; Kuwata, S.; Ueno, K.; Shiro, M.; Hidai, M. *Angew. Chem., Int. Ed.* **2000**, *39*, 1128−1131.
(21) Nagano, T.; Kuwata, S.; Ishii, Y.; Hidai, M. *Organometallics* **2000**, *19*, 4176−4178.
(22) Kuwata, S.; Kabashima, S.; Sugiyama, N.; Ishii, Y.; Hidai, M. *Inorg. Chem.* **2001**, *40*, 2034−2040.
(23) Kuwata, S.; Nagano, T.; Matsubayashi, A.; Ishii, Y.; Hidai, M. *Inorg. Chem.* **2002**, *41*, 4324−4330.
(24) Kuwata, S.; Hashizume, K.; Mizobe, Y.; Hidai, M. *Organometallics* **2002**, *21*, 5401−5407.
(25) Seino, H.; Mizobe, Y.; Hidai, M. *New J. Chem.* **2000**, *24*, 907−911.
(26) Takagi, F.; Seino, H.; Mizobe, Y.; Hidai, M. *Organometallics* **2002**, *21*, 694−699.
(27) Kato, H.; Seino, H.; Mizobe, Y.; Hidai, M. *J. Chem. Soc., Dalton Trans.* **2002**, 1494−1499.
(28) Takagi, F.; Seino, H.; Hidai, M.; Mizobe, Y. *J. Chem. Soc., Dalton Trans.* **2002**, 3603−3610.
(29) Kato, H.; Seino, H.; Mizobe, Y.; Hidai, M. *Inorg. Chim. Acta* **2002**, *339*, 188−192.
(30) Nagao, S.; Seino, H.; Hidai, M.; Mizobe, Y. *J. Organomet. Chem.* **2003**, *669*, 124−134.

Scheme 8. Reaction of **4** with Hydroxyl- and Bromoalkenes

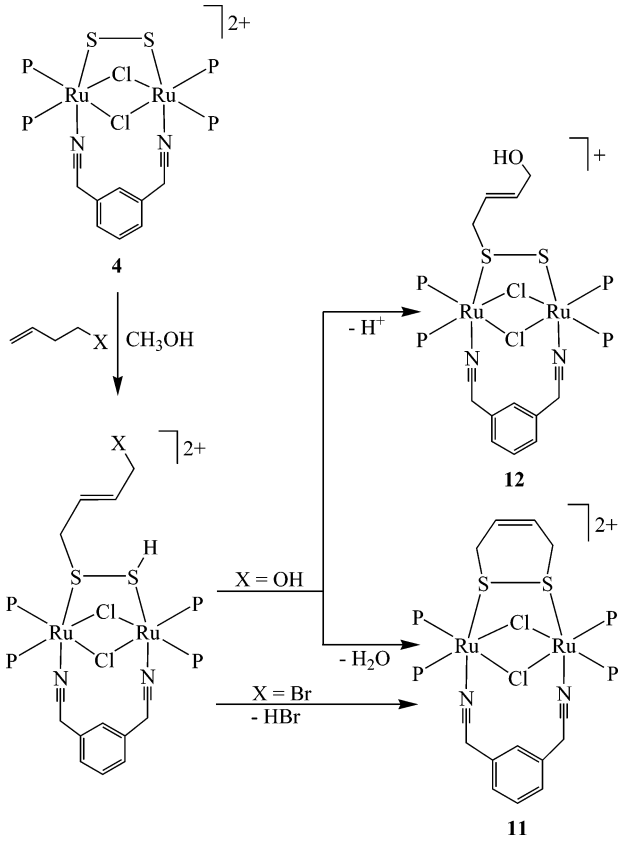

ated C−C bond is well known.[35−41] Unlike these other complexes, **3** does not have such a hydrosulfido moiety. However, in the initial step of the alkene and alkyne reactions, **3** generates a hydrosulfido moiety, in which the hydrogen atom is immediately trapped by the unsaturated C−C bond. The disulfido ligand of **4** could also cleave a C−H bond to form an intermediate between **4** and **7** or **8** in Scheme 5. However, the hydrodisulfido ligand eliminates a H^+ to give **7** or undergoes condensation with CH_3OH to give **8** instead of hydrogen addition to the C═C bond. The formation of **8** strongly supports the formation of a S−H bond after C−H bond activation. Similarly, the reaction of **4** with 1-hexene gave **5**, **9**, and **10**. It is noteworthy that the

(31) Sinozaki, A.; Seino, H.; Hidai, M.; Mizobe, Y. *Organometallics* **2003**, *22*, 4636−4638.
(32) Wang, W.-D.; Guzei, I. A.; Espenson, J. H. *Inorg. Chem.* **2000**, *39*, 4107−4112.
(33) Ruiz, J.; Rodriguez, V.; Vicente, C.; Marti, J. M.; Lopez, G.; Perez, J. *Inorg. Chem.* **2001**, *40*, 5354−5360.
(34) Chatwin, S. L.; Diggle, R. A.; Jazzar, R.; Rodolphe, F. R.; MacGregor, S. A.; Mahon, M. F.; Whittlesey, M. K. *Inorg. Chem.* **2003**, *42*, 7695−7697.
(35) Casewit, C. J.; Coons, D. E.; Wright, L. L.; Miller, W. K.; Rakowski DuBois, M. *Organometallics* **1986**, *5*, 951−955.
(36) Birnbaum, J.; Laurie, J. C. V.; Rakowski DuBois, M. *Organometallics* **1990**, *9*, 156−164.
(37) Kuwata, S.; Andou, M.; Hashizume, K.; Mizobe, Y.; Hidai, M. *Organometallics* **1998**, *17*, 3429−3436.
(38) Buil, M. L.; Elipe, S. E.; Esteruelas, M. A.; Oñate, E.; Peinado, E.; Ruiz, N. *Organometallics* **1997**, *16*, 5748−5755.
(39) Kaiwar, S. P.; Hsu, J. K.; Liable-Sands, L. M.; Rheingold, A. L.; Pilato, R. S. *Inorg. Chem.* **1997**, *36*, 4234−4240.
(40) Kaneko, Y.; Suzuki, T.; Isobe, K. *Organometallics* **1998**, *17*, 996−998.
(41) Takagi, F.; Seino, H.; Mizobe, Y.; Hidai, M. *Can. J. Chem.* **2001**, *79*, 632−634.

Table 3. Selected Bond Distances (angstroms), Angles (deg), and Torsion Angles (deg) of **6** and **11**

	6-Cl	6-Br	11
	Bond Distances		
Ru1−S1	2.325(2)	2.305(3)	2.3096(10)
Ru2−S2	2.313(2)	2.305(3)	2.3281(11)
Ru1−P1	2.221(2)	2.221(3)	2.2156(11)
Ru1−P2	2.230(2)	2.217(3)	2.2273(11)
Ru2−P3	2.219(2)	2.215(3)	2.2201(11)
Ru2−P4	2.222(2)	2.229(3)	2.2351(11)
Ru1−N1	2.058(7)	2.033(9)	2.041(3)
Ru2−N2	2.043(7)	2.032(9)	2.048(3)
Ru1−X1	2.489(2)	2.6010(17)	2.5307(9)
Ru1−X2	2.505(2)	2.5780(15)	2.5194(9)
Ru2−X1	2.514(2)	2.6065(15)	2.4975(9)
Ru2−X2	2.507(2)	2.5818(15)	2.5145(10)
S1−S2	2.091(3)	2.165(3)	2.1044(14)
S1−C23	1.808(8)	1.830(11)	1.815(4)
S2−C26	1.799(8)	1.842(11)	1.816(4)
C23−C24	1.498(11)	1.494(15)	1.510(6)
C24−C25	1.328(11)	1.329(16)	1.324(7)
C25−C26	1.515(10)	1.476(16)	1.508(6)
C24−C27	1.520(10)	1.496(16)	
C25−C28	1.490(11)	1.484(15)	
	Bond Angles		
S1−S2−Ru2	104.41(10)	109.57(13)	103.81(5)
S2−S1−Ru1	103.85(10)	109.62(13)	104.91(5)
S1−Ru1−N1	168.35(18)	172.0(2)	168.02(10)
S2−Ru2−N2	168.05(19)	172.6(2)	170.02(10)
Ru1−X1−Ru2	93.03(7)	90.91(4)	92.60(3)
Ru1−X2−Ru2	92.81(7)	91.99(4)	92.47(3)
X1−Ru1−X2	80.74(7)	83.52(4)	80.09(3)
X1−Ru2−X2	80.19(7)	83.33(5)	80.82(3)
S1−S2−C26	94.1(3)	98.9(4)	94.61(15)
S2−S1−C23	93.4(3)	99.1(4)	94.86(15)
S1−C23−C24	114.0(6)	110.5(8)	109.4(3)
S2−C26−C25	113.2(6)	109.4(8)	111.7(3)
C23−C24−C25	128.0(7)	118.8(10)	128.0(4)
C24−C25−C26	125.1(7)	117.9(10)	129.2(4)
	Torsion Angles[a]		
Ru1−S1−S2−Ru2	43.59(11)	1.94(16)	42.28(5)
C23−C24−C25−C26	4.8(14)	1.3(16)	2.3(8)

[a] Reported without the sign.

$Ru^{II}Ru^{III}$ **5** is always formed in the reactions with terminal alkenes. Analogous reduction was observed in the reactions of **3** with less reactive substrates. For the formation of **5**, both of the alkenyl and hydrogen groups on the disulfido ligand are probably released as a cation and a radical, that is, a proton and an alkenyl radical or an H radical and an alkenyl cation. Similarly, **3** is gradually reduced to the isostructural $Ru^{II}Ru^{III}$ complex in a CH_3CN solution,[2] and when the reaction with the substrate is slower than the reduction reaction, the reduced product is dominantly formed. Another possible explanation is that although the C−S formation occurs, the decomposition of the complex via C−S bond cleavage causes the reduction reaction to occur. However, **2** is not reduced at room temperature under the usual reaction conditions. In summary, **3** and **4**, which react to form a C−S bond, are easily reduced to the $Ru^{II}Ru^{III}$ complexes, whereas **2**, which does not react to form a C−S bond, is resistant to the reduction.

Although **4** can react with internal alkenes, **3** does not react with internal alkenes, except with cyclohexene.[5] The reaction of **4** with 2-pentene gave **5** as the major product and a trace amount of **8**. The reaction of **4** with 2-hexene gave complex **10**, which has a C−S bond, and free 3-hexene, Scheme 7. It

Table 4. Selected Bond Distances (anstroms), Angles (deg), and Torsion Angles (deg) of **7**−**10** and **12**

	7	**9**	**12**	**8**	**10**
			Bond Distances		
Ru1−S1	2.355(2)	2.361(2)	2.352(3)	2.324(2)	2.342(3)
Ru2−S2	2.352(2)	2.360(3)	2.342(3)	2.340(2)	2.338(3)
Ru1−P1	2.233(2)	2.229(2)	2.217(3)	2.2194(19)	2.226(3)
Ru1−P2	2.216(2)	2.230(2)	2.202(3)	2.222(2)	2.243(3)
Ru2−P3	2.197(2)	2.219(3)	2.196(3)	2.222(2)	2.227(3)
Ru2−P4	2.223(3)	2.222(3)	2.225(4)	2.234(2)	2.221(3)
S1−S2	2.066(3)	2.072(3)	2.039(5)	2.116(3)	2.116(4)
S1−C^{α}	1.862(10)	1.845(9)	1.948(16)	1.821(8)	1.823(11)
C^{α}−C^{β}	1.532(13)	1.528(17)	1.60(2)	1.537(17)	1.59(3)
C^{β}−C^{γ}	1.331(16)	1.38(2)	1.24(3)	1.365(18)	1.30(4)
C^{γ}−C^{δ}	1.502(17)	1.48(2)	1.51(4)	1.526(18)	1.48(4)
S2−C^{Me}				1.805(8)	1.827(13)
			Bond Angles		
S1−S2−Ru2	106.42(10)	106.42(11)	106.85(14)	104.91(9)	104.82(8)
S2−S1−Ru1	108.11(9)	108.53(11)	106.85(14)	104.82(8)	104.46(14)
S2−S1−C^{α}	98.5(4)	100.4(3)	94.2(7)	100.1(3)	99.9(4)
S1−C^{α}−C^{β}	109.1(6)	107.6(8)	108.7(10)	108.3(7)	105.1(11)
C^{α}−C^{β}−C^{γ}	122.2(12)	120.6(13)	122(3)	122.6(13)	127(3)
C^{β}−C^{γ}−C^{δ}	125.9(15)	126.3(19)	122(3)	120.3(15)	131(4)
S1−S2−C^{Me}				99.8(3)	99.9(5)
			Torsion Angles[a]		
Ru1−S1−S2−Ru2	24.85(14)	22.85(14)	21.9(2)	36.93(10)	37.69(16)
Ru2−S2−S1−C^{α}	90.2(3)	93.4(4)	90.6(4)	156.2(3)	156.2(3)
Ru1−S1−S2−C^{Me}				155.1(3)	157.2(5)
C^{α}−C^{β}−C^{γ}−C^{δ}	175.0(10)	179.8(13)	179.1(16)	177.6(11)	177.6(11)

[a] Reported without the sign.

Table 5. Summary of the S−S Bond Distances and Ru−S−S−Ru Angles

compound	no. of C−S bonds	S−S (Å)	Ru−S−S−Ru (deg)	S−S (Å) from **3**
4-Cl	0	1.974(4)	1.6 (2)	1.933(11)
5-Cl	0	1.995(3)	12.16(15)	1.995(3)
7	1	2.066(3)	24.85(14)	
9	1	2.072(3)	22.85(14)	
12	1	2.039(5)	21.9(2)	
6-Cl	2	2.091(3)	43.59(11)	2.093(5)
11	2	2.1044(14)	42.28(5)	−2.099(3)
8	2	2.116(3)	36.93(10)	
10	2	2.116(4)	37.69(11)	

is possible that isomerization also occurred in the case of 2-pentene; however, the product is the same as the starting material. In addition, on the basis of the reaction with internal alkenes, isomerization may also occur when a terminal alkene is used, to form 1-pentene and 1-hexene, which can react with the disulfido ligand. Scheme 7 shows a plausible summary of the events in the reaction of **4** with 2-alkenes. Although the reason why is not clear, the C−S bond involving a carbon atom in the chain, that is, not the terminal C atom, appears unstable.

The reactions giving **8** and **10** are examples of intermolecular dehydration, in which the first molecule (alkene) provides a proton and the second molecule (CH_3OH) provides a hydroxyl group, eliminating one molecule of H_2O. An analogous reaction has been found for the tetracationic **3**;[38] however, it usually involves homocoupling. Previously, the cross-coupling of propargyl alcohol and 2-butyn-1-ol was reported.[42] However, these substrates are not significantly different. Therefore, the reactions affording **8** and **10** are unique. In contrast, intramolecular elimination is common for **3** and **4**.[43] Treatment of **4** with 4-bromo-1-butene results in the formation of the C_4S_2 six-membered ring complex $[\{Ru(P(OCH_3)_3)_2\}_2(\mu\text{-}SCH_2CH{=}CHCH_2S)(\mu\text{-}Cl)_2\{\mu\text{-}C_6H_4(CH_2CN)_2\}](CF_3SO_3)_2$ (**11**) via intramolecular elimination of HBr. The reaction of **4** with 3-butene-1-ol gives the same C_4S_2 six-membered ring (**11**) and $[\{Ru(P(OCH_3)_3)_2\}_2(\mu\text{-}SSCH_2CH{=}CHCH_2OH)(\mu\text{-}Cl)_2\{\mu\text{-}C_6H_4(CH_2CN)_2\}](CF_3SO_3)$ (**12**), which has one C−S bond and a 1+ charge. These reactions suggest that the hydrogen atom of the hydrodisulfido ligand reacts as an acid, and H_2O or HBr are eliminated (Scheme 8).

Structural Study. 4−**12** were characterized by X-ray diffraction as well as NMR and ESI-MS spectroscopy. The structure of **4** is shown in Figure 1. The structural parameters of **4** and **5** are summarized in Table 2. The structure of **5** is similar to **4**, and therefore, the ORTEP diagram is not shown. In both complexes, the ruthenium atoms are bridged by *m*-xylylenedicyanide, of which the cyanide nitrogen atoms coordinate trans to the disulfido ligand. The S−S bond distances of Ru^{III}_2 complexes **4-Cl** and **4-Br** are almost equal (1.974(4) Å and 1.9726(19) Å, respectively) and are also comparable to those of previously reported disulfido complexes $[\{Ru(P(OCH_3)_3)_2(CH_3CN)\}_2(\mu\text{-}S_2)(\mu\text{-}Cl)_2]^{2+}$ (**2**) (1.973(7) Å) and $[\{Ru(P(OCH_3)_3)_2(CH_3CN)_3\}_2(\mu\text{-}S_2)]^{4+}$ (**3**) (1.933(11) Å). The $Ru^{II}Ru^{III}$ mixed valence complexes **5-Cl** and **5-Br** have slightly longer S−S distances (1.995(3) Å and 2.0131(18) Å, respectively) than those of the Ru^{III}_2 complexes. Having larger ionic radii, the two bromine atoms in **4-Br** can exert larger steric repulsion than the chlorine atoms in **4-Cl**, which may cause the cation to expand in the

(42) Matsumoto, K.; Moriya, Y.; Sugiyama, H.; Hossai, M. M.; Lin, Y.-S. *J. Am. Chem. Soc.* **2002**, *124*, 13106−13113.

(43) Hatemata, S.; Sugiyama, H.; Sasaki, S.; Matsumoto, K. *Inorg. Chem.* **2002**, *41*, 6006−6012.

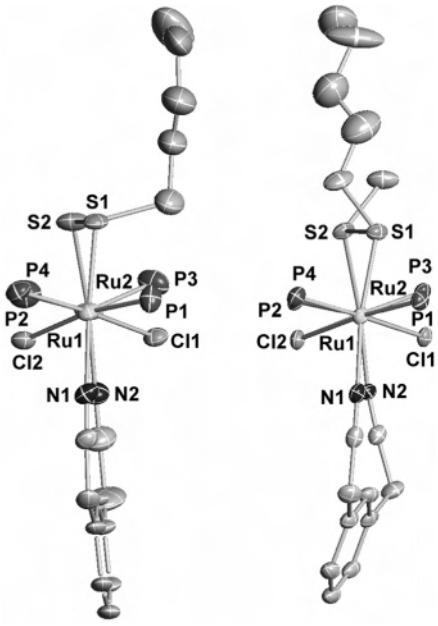

Figure 6. Side views of **7** and **8**. The OCH_3 groups are omitted for clarity.

direction perpendicular to the RuSSRu core plane. This repulsion causes a narrower Ru−Br−Ru angle and a wider Br−Ru−Br angle in **4-Br** than those in **4-Cl**.

The structures of **6-Cl** and **6-Br** are shown in Figures 2 and 3, respectively, and selected bond distances and angles of **6** are summarized together with those of **11** in Table 3, in which the C23 to C26 atoms are common to the C_4S_2 rings of all three complexes. Atoms C27 and C28 are the methyl carbon atoms at the β and γ positions in **6**. The distances clearly show that the C_4S_2 ring has a C═C double bond (1.328(11), 1.329(16), and 1.323(7) Å for **6-Cl**, **6-Br**, and **11**, respectively) and a relatively long S−S bond (2.091(3), 2.165(3), and 2.1044(14) Å for **6-Cl**, **6-Br**, and **11**, respectively). Although the S−S bond distances in the starting complexes **4-Cl** and **4-Br** are comparable, the S−S bond in **6-Br** is significantly longer than those of **6-Cl** and **11**. The different conformations of the C_4S_2 rings, that is, complexes **6-Cl** and **11** have chair type conformations (Figure 2) and **6-Br** has a boat-type conformation (Figure 3), can cause the different S−S bond distances.

Selected bond distances and angles for **7**−**10** and **12** are summarized in Table 4, and the alkenyl C atoms are listed

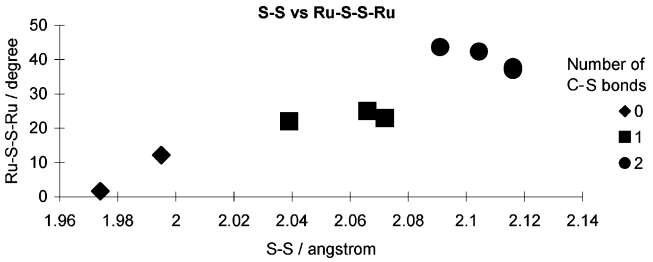

Figure 7. Plot of the S−S bond distances versus the Ru−S−S−Ru angle.

from C^{α} to C^{δ} because they are common for each complex. Figures 4 and 5 show the structures of **7** and **8**, respectively. **8** has a methyl group on the disulfide. **8** and **10** with alkenyl methyl disulfido ligands have significantly longer S−S bond distances and larger Ru−S−S−Ru torsion angles compared to those of the alkenyl disulfido complexes because of the steric hindrance between alkenyl and methyl groups. In addition, the Ru2−S2-S1−C^{α} torsion angles of the alkenyl disulfido (90°) and alkenyl methyl disulfido (156°) complexes are significantly different and this difference is clearly observed in the side views of **7** and **8** in Figure 6. **6-Cl** and **11** have shorter S−S bonds compared to those of **8** and **10** because the S−S bonds within the six-membered C_4S_2 rings are constrained.

Table 5 summarizes the relation between the number of C−S bonds, the S−S bond distances, and the Ru−S−S−Ru torsion angles for the chloride-bridged complexes. A plot of the S−S bond distance versus the Ru−S−S−Ru torsion angle is shown in Figure 7. There is a good correlation between the parameters. Previously, we analyzed the C−S bond formation products of **3** in the same manner, and the S−S bond distances are comparable to those in the present study.[44]

Acknowledgment. This research was supported by the Ministry of Education, Culture, Sports, Science, and Technology (MEXT), (the 21st Century COE program).

Supporting Information Available: ESI-MS of **8** prepared in CH_3OH and CD_3OD. ^{31}P NMR spectra of **9** at 293 and 273 K. ^{1}H NMR of **4-Cl** in CD_3CN. This material is available free of charge via the Internet at http://pubs acs.org.

IC062460K

(44) Matsumoto, K.; Sugiyama, H. *Acc. Chem. Res.* **2002**, *35*, 915−926.